齐鲁工业大学
QILU UNIVERSITY OF TECHNOLOGY

本科毕业设计（论文）

A Novel Fluorescent Sensor for Ultra-sensitive Detection of Al^{3+} and its Bioimaging Application in Living Cells

学院名称　化学与制药工程学院

专业班级　16-1 应用化学（国际班）

学生姓名　徐长岭

学　　号　201604301182

导师姓名　牛庆芬

2020 年　　5 月　　20 日

A novel fluorescent sensor for ultra-sensitive detection of Al^{3+} and its bioimaging application in living cells

一种超灵敏检测铝离子的荧光探针及在活细胞中生物成像的应用

学院名称 化学与制药工程学院

专业班级 应化（全英语）15-1

学生姓名 徐长岭

学号 201604301182

导师姓名 牛庆芬

专业技术职务 副教授

齐鲁工业大学本科毕业论文原创性声明

本人郑重声明：所呈交的毕业论文，是本人在指导教师的指导下独立研究、撰写的成果。论文中引用他人的图件、数据、资料、文献，均已在论文中加以说明，除此之外，本论文不含任何其他个人或集体已经发表或撰写的成果作品。对本文研究做出重要贡献的个人和集体，均已在文中作了明确说明并表示了谢意。本声明的法律结果由本人承担。

毕业论文作者签名：徐长岭

年　　月　　日

齐鲁工业大学关于毕业论文使用授权的说明

本毕业论文作者完全了解学校有关保留、使用毕业论文的规定，即：学校有权保留、送交论文的复印件，允许论文被查阅和借阅，学校可以公布论文的全部或部分内容，可以采用影印、扫描等复制手段保存本论文。

指导教师签名：　　毕业论文作者签名：徐长岭

年　　月　　日　　年　　月　　日

Contents

Abstract.....1
摘要.....2
Chpter1 Introduction.....3
1.1 Background.....3
1.2 Introduction of fluorescence spectrum.....4
1.3 Design principle of fluorescent probes.....5
1.4 Recognition mechanism of fluorescent probes.....6
1.4.1 Intramolecular Charge Transfer (ICT).....6
1.4.2 Fluorescence Resonance Energy Transfer (FRET).....7
1.4.3 Photo-Induced Electron Transfer (PET).....8
1.4.4 Aggregation-Induced Emission (AIE).....9
1.5 Thiophene-based aluminium fluorescent sensor.....9
1.6. Subject Research.....10
1.6.1 Purpose of the Project.....10
1.6.2 Research contents.....10
1.6.3 Synthetic route.....10
Chapter 2 Experimental Section.....11
2.1 Experimental objective.....11
2.2 Characterization methods.....11
2.3 Reagents and Apparatus.....11
2.3.1 Apparatus.....11
2.3.2 Reagents.....13
2.4 Experiment Contents.....14
2.4.1 preparation of testing solution.....14
2.4.2 Cell culture.....14
2.4.3 Synthesizing of TSA.....14
Chapter 3 Result and discussion.....18
3.1 High Fluorescence selectivity to Al^{3+}.....18
3.2 Anti-interference performance of TSA.....19
3.3 The sensitivity of TSA to Al^{3+}.....20
3.4 Limited of detection of TSA-Al^{3+}.....21
3.5 Calculation of the binding association constant.....22
3.6 pH Responses of Sensor TSA to Al^{3+}.....23
3.7The time response of TSA to Al^{3+}.....24
3.8 Cell imaging study.....25
Chapter 4 Conclusion.....26
Bibliography.....27
Acknowledgments.....29

Abstract

After the late 20th century, with the continuous development of industrialization worldwide, environmental pollution issues put a huge burden on society and living organisms. Many excessive metal ions have been found in humans and animals, as well as in the environment. It caused huge damage to functional organisms. For example, transitional metal ions Al^{3+}, Cu^{2+} and other metal ions were considered a contributor to cancer. Thus, it is necessary to develop an efficient and convenient sensor for rapid detection of metal ions. In this work, a novel fluorochrome based on thiophene Schiff base has been synthesized and investigated for ultrasensitive detection of Al^{3+} and its bioimaging application in living cells.with high selectivity and anti-interference over other metal ions, the TS displayed a very fast fluorescence-enhanced response towards Al^{3+} and with low detection limits TS (3.7 nM for Al^{3+}) and wide pH response range TS (4.0–12.0) high stability TS (binding constant $1.16\times10^{4}M^{-1}$). The sensing mechanism between Al^{3+} and TS was investigated, and the result shows that the chemical binding stoichiometric ratio of TS-Al^{3+} is 1:1. Importantly, experiments of TS-Al^{3+} have carried out in various environmental solutions and coated paper strips, and it worked well. More importantly, it can be used in living cells detection of Al^{3+}, which granted its potential application in bioimaging.

Key words: Fluorochrome； Thiophene Schiff-base； Al^{3+}； bioimaging application

摘 要

由于在20世纪中后期世界范围内工业化的持续不断的发展，环境污染问题已经给人类社会和生命造成了沉重负担和后果。在人类，动物以及环境中发现了许多过量的金属离子，这对生物的正常的器官造成了巨大破坏。例如，过渡金属离子Al^{3+}，Cu^{2+}和其他金属离子被认为是导致癌症的原因之一。因此，开发一种用于快速检测相应的金属离子的高效便捷的传感器就是非常有必要的。在我的这项工作中，我们合成并研究了一种基于噻吩席夫碱的新型荧光染料，用于Al^{3+}的超灵敏检测及其在活细胞中的生物成像应用。TSC具有对其他金属离子的高选择性和抗干扰性，显示出非常快的荧光-对Al^{3+}的响应增强，检测限TSC（Al^{3+}为3.7 nM）和pH响应范围TS（4.0-12.0）宽，稳定性高（结合常数1.16×104M^{-2}）。研究了Al^{3+}与TSC之间的感应机理，结果表明TSC-Al^{3+}的化学结合化学计量比为1:1。重要的是，TS-Al^{3+}的实验已在各种环境解决方案和涂布纸带中进行，并且效果良好。更重要的是，它可用于Al^{3+}的活细胞检测，这使其在生物成像中具有潜在的应用前景。

关键词： 荧光传感器　噻吩希夫碱　铝离子　生物成像

Chapter 1 Introduction

1.1. Background

For many countries, especially in developing countries, they are producing a severe and huge amount of pollution while manufacturing, on the way of industrialization. The pollutants discharged by industry, that nature cannot process it or exceeds its processing capacity, which leads to very serious environmental damage and eventually causes human illness. For example, The discharge of waste liquid containing high concentration metal ions has a significant impact on the entire ecosystem. Those unqualified emit of chemical and industrial harmful metal ions (Al^{3+}, Fe^{3+}, Ag^{+}, Cu^{2+}, Hg^{2+}, Pb^{2+}) can negatively affect the environment and individuals though some of them (Fe^{3+}, Li^{+}, K^{+}, Mg^{2+}, Ca^{2+} , etc) that are indispensable elements in living organisms, and maintaining their stable operation in the living organisms and related systems has well considered. Thus, it is necessary to keep a proper level of these essential trace elements[1].

Aluminium exist in many forms, and is considered the most plentiful metallic element in the earth's crust[2]. Aluminium is considered to cause severe damage to the central nervous system and immune system of the human body, and affect the absorption and use of other trace elements. Principal sources of Al^{3+} contamination in human beings are food additives, aluminium-based pharmaceuticals, occupational dust, aluminium containers, cooking utensils, paper industry, dye production and the textile industry. Some health hazards such as Alzheimer's disease, Parkinson's disease, amyotrophic lateral sclerosis, etc[3] was authenticated that they can be caused by excess intake of aluminium ions of human body. Therefore, the achievable detection of Al^{3+} ions and others for environmental monitoring and biological research had became a central discussion[4]. According to the report from United Nations World Health Organization, the aluminum ion concentration in drinking water was supposed to be below 200 mg / L, and the maximum aluminum intake per 1Kg of human body

weight should not exceed 7 mg per week[5]. The atomic absorption spectroscopy, inductively coupled plasma-mass spectrometry, inductively coupled plasma atomic emission spectrometry were most used in element identification (aluminium detection), but they are very complex and not bio-available, as the chemo-sensor does[6].

Many fluorescent probes contain three five-membered heterocyclic structural units, pyrrole, furan, or thiophene. They all contain six π electrons, and according to the Hückel rule, they are all aromatic. The electron cloud density of the thiophene is higher than that of the other two, which gives it unique optical properties and electron transmission capabilities. Besides, thiophene compounds have been widely used in drug design, dye chemistry, diagnostics, electronic and optoelectronic devices, self-assembled supramolecular structures, and sensing devices due to its advantages of high chemical stability and easy synthesis[7]. In recent years, fluorescence spectroscopy has caused great interest among researchers worldwide due to its low detection limit, high selectivity and sensitivity, simple instrumentation, operational available and the capacity for rapid and real-time monitoring and potential application in living cells[7]. Some fluorescent probe can effective detect the Al^{3+} have been reported, but improving their water solubility and lower their cell toxicity still is a important research field. In addition, in this work, a novel type of thiophene fluorescent probe TSA was designed and synthesized for dealing with those troubles.

1.2. Introduction of fluorescence spectrum

Fluorescence refers to the emission of molecules and atoms in the excited state(S_2, S_1/T_2, T_1) when they return to the ground state(S_0), the same as phosphorescence[8]. They are luminescence that differs in singlet and triplet state, and most compounds are in singlet of their ground state. Fluorescent probes are fluorescent molecules that have the characteristic fluorescence in the ultraviolet, visible, and infrared regions and changes sensitively with the environment.（excited and emission wavelength, aqueous solution etc） Normally speaking, it consists of

three parts, fluorophore, spacer, receptor. Many different types of Fluorescent probes have been discovered and developed differently in the three parts. They intersected with other subjects fields (medicine, physics, biology) and research and widely used in biological indicators, fluorescent dyes, fluorescent labels, and intracellular imaging[9].

Photoluminescence(PL), fix the wavelength of the emitted light and record the change of fluorescence intensity with the emission wavelength. Photoluminescence Excitation(PLE), fix the wavelength of emitting light, change the wavelength of excitation light, and record the change of fluorescence intensity with the excitation wavelength. What they recorded was the change of fluorescence intensity with wavelength. So the vertical coordinate of the fluorescence spectrum is the intensity and the horizontal coordinate is the wavelength. In addition, the peak position and half peak width can be obtained from the graph and the peak position directly reflects the color of fluorescence while the half peak width represents the purity of fluorescence. But for the Fluorescence absorption spectrum, the vertical coordinate is the absorbance.

1.3. Design principle of fluorescent probes

There are different types of fluorescent probes, but the goal is to detect the analyte, whatever for the complex, or reaction fluorescent probes.Both the combined (Figue 1) and displacement (Figue 2) types of fluorescent probes are consist of three parts, fluorophore, spacer, receptor. For the combined type of fluorescent probes, it will present the signal changes (stoke shift and color change) after it responded to the target while the other one will release the indicator contributed to the displacement of the target. What more, some fluorescent probes can react with the target and generate new substances, thus display differences[10].

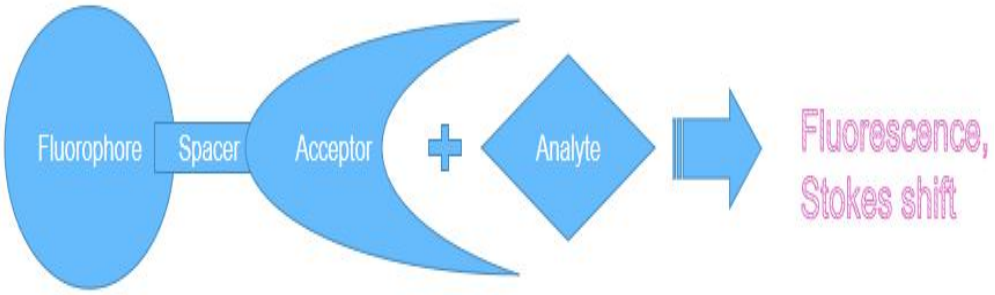

Figure. 1-1 Combine type of fluorescent probe

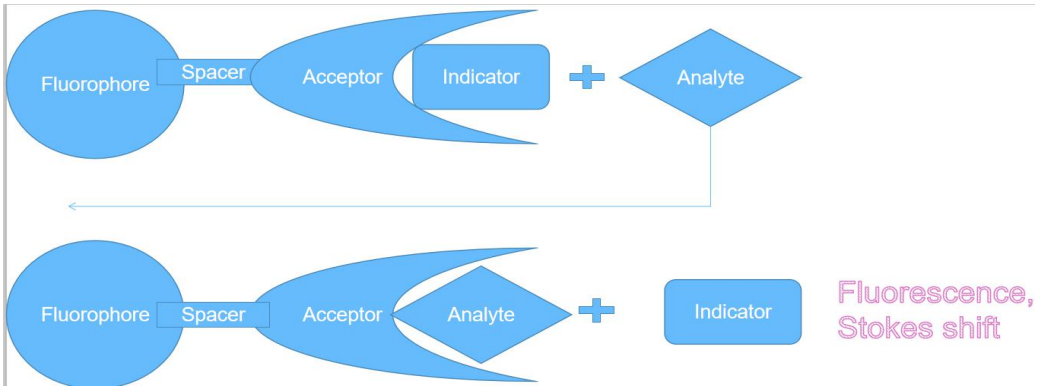

Figure. 1-2 Displacement type of fluorescent probe

1.4. Recognition mechanism of fluorescent probes

The recognition mechanism of fluorescent molecular probes mainly includes intramolecular charge transfer (ICT), fluorescence resonance energy transfer (FRET), photo-induced electron transfer (PET), aggregation-induced emission (AIE), etc[11].

1.4.1 Intramolecular Charge Transfer (ICT)

The typical ICT fluorescent probe is a strong push-pull electron system, which is connected with the strong (push) electron donor group and the (pull) electron-withdrawing group respectively in the fluorophore. The push electron group is conjugated with the pull electron group in ICT. Under the excitation of light with specific wavelength, the charge transfer from the electron donor to the electron acceptor will occur.

In 2014, Lin Yang, Xiao Zhang and others designed and synthesized two

chemodosimeters PDMI and PMI for cyanide detection that based on phenazine-cyanine dyes with N-methyl indolium group as receptor unit.The quenching effect on phenazine-cyanine fluorophore caused by strong intramolecular charge transfer (ICT). After the addition of cyanide, the ICT effect decreased and vanished leading to dramatic "off–on" fluorescence enhancement. both of the compound PDMI and PMI are high sensitivity (detection limit of 1.4 μM and 200 nM, respectively) and high selectivity against other anions[12, 13] .

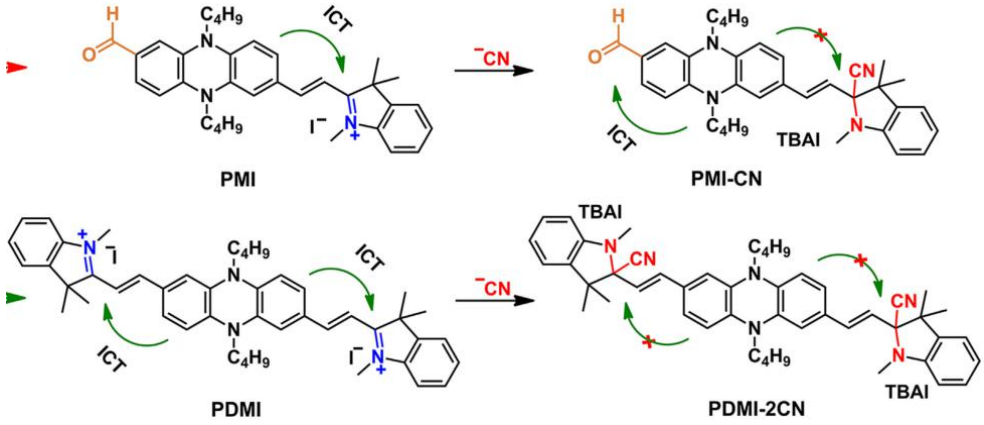

Figure.1- 3 ICT mechanism of PMI and PDMI (ICT)

1.4.2 Fluorescence Resonance Energy Transfer (FRET)

Fluorescence resonance energy transfer happened in two fluorophore, which is a nonradiative transfer of energy from an excited donor fluorophore to a ground-state acceptor fluorophore within proximity (normally 1–10 nm) via long-range dipole-dipole interactions. The FRET process highly depends on the degree of spectral overlap between donor fluorescence emission and acceptor absorption. The process is also sensitive towards the donor-acceptor separation distance and their relative dipole orientations[17]. In 2012, Yunlong Liu, and his teammates successfully synthesized a fluorescent probe for Hg^{2+} recognition based on fluorescence resonance energy transfer. It based on the Hg^{2+} promoted desulfurization reaction and displayed excellent selectivity and high sensitivity toward detecting Hg^{2+}. The large Stokes shift

(185 nm) can be realized in the system. More importantly, the detection limit can low to 3×10^{-8} M [14].

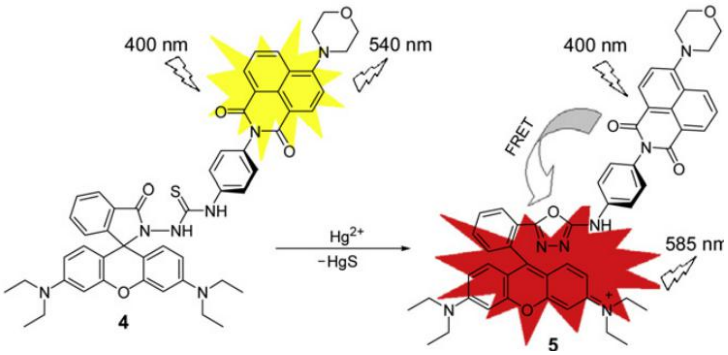

Figure. 1-4 FRET mechanism of FRET

1.4.3 Photo-Induced Electron Transfer (PET)

Photoinduced electron transfer probes are generally composed of fluorophores, spacer, and electron recognition groups. The mechanism is that the electron transition from HOMO to LUMO takes place after the fluorophore is excited by light irradiation, the energy of the electron donor group is higher than that of the HOMO of the fluorophore, which leads to the HOMO electron transition from the electron donor group to the electron acceptor group (fluorophore). Therefore, the excited electrons of the fluorophore cannot back to the ground state to release energy, thus resulting in quenching of emission. When the detection target is combined with the recognition group, the electron providing capacity of the donor group will decrease, and the photo-induced electron transfer process is blocked. Thus the excited electrons of the fluorophore can return to the ground state, and the fluorescence is restored[15].

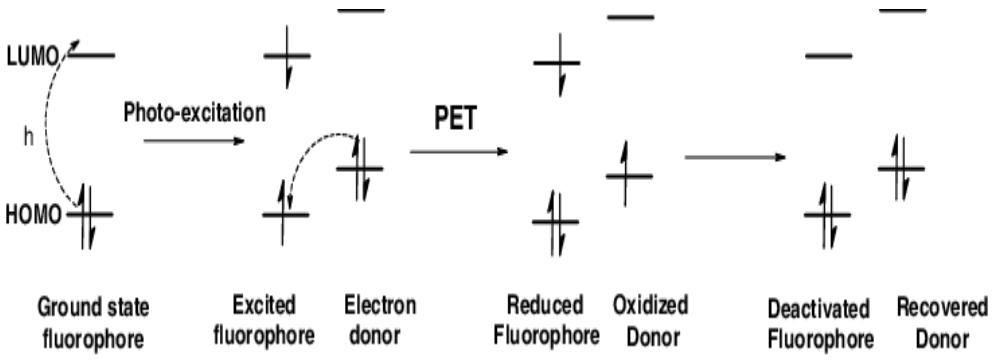

Figure. 1-5 PET mechanism

1.4.4 Aggregation-Induced Emission (AIE)

The concept of aggregation-induced emission (AIE) was first raised by Tang‘s group in 2001. Normally speaking, conventional aromatic luminophores have aggregation-caused quenching (ACQ) effect, where the excited states of the aggregates often relax back to the ground state via non-radiative channels, resulting in the quenching of emission. But, Tetraphenylethene (TPE), as one of the prototypical AIE luminophores, is exactly opposite to the ACQ process.

In 2019, Fan Wang, Xu Zeng, and others synthesized a fluorescent compound Tetra(3-[benzoylhydrazone] methyl-4-hydroxyphenyl) ethane for sensing of Al^{3+} based on the aggregation-induced emission (AIE). selectively enhanced with Al^{3+} by blocking the photo-induced electron transfer (PET) process, and locking the isomerization of C=N bond and the intramolecular rotation around this C=N bond[16].

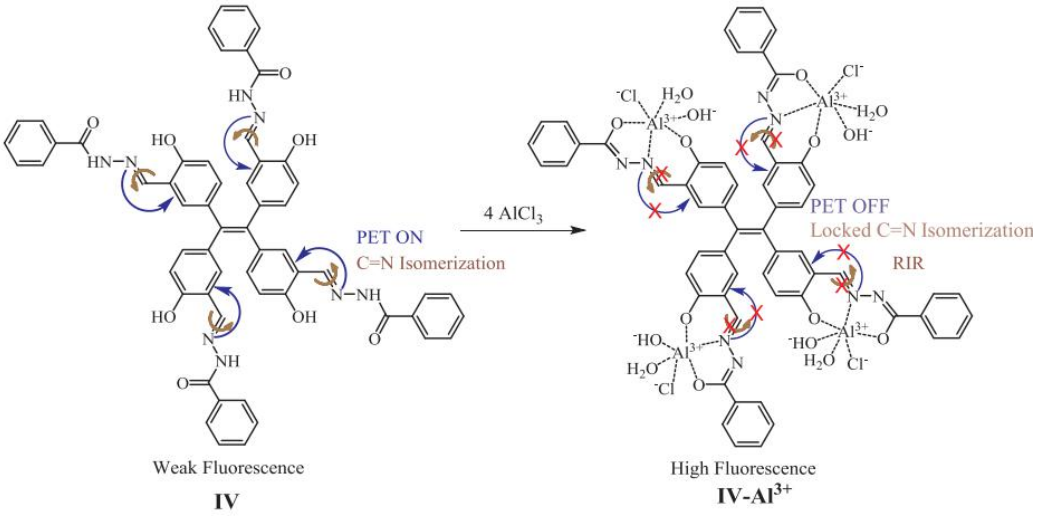

Figure.1-6 AIE mechanism of IV for detection of Al^{3+}

1.5 **Thiophene-based fluorescent probe**

A fluorescent sensor, which should have a high quantum yield, large stokes shift, fast response time, and excellent photostability, is widely used for metal ions detection and cell imaging. Thiophene-based Fluorophores have been widely used as organic dyes for efficient fluorescent cell staining, labeling of proteins and DNA. This widespread use resulting from the high photo-stability of the fluorophore skeleton, low cytotoxicity, high color-tunable emission, high quantum efficiency and large Stokes shifts[17].

Figure.1-7 Thiophene

1.6 **Research**

1.6.1 Purpose of the Project

Metal ions are ubiquitous in our lives. Taking harmful or excessive metal ions will hurt the human body. Therefore, it is very urgent to detect these metal ions efficiently and effectively in various living environments. In my lab-work, a new

thiophene Schiff base (**TSA**) was designed, and its structure and sensing performance were characterized, and its detection ability for Al^{3+} was analyzed.

1.6.2 Research contents

Thiophene has the strong points of good charge transfer performance and strong electron supply performance. In this work, thiophene is used as the electron supply unit to design and synthesize a new type of organic small molecule fluorescence sensor material. After synthesizing, the structure of the synthetic fluorescent probe was characterized by NMR, FTIR, MS and UV-visible spectrometry, which consistent with the designed structure. The selectivity, competition, job's lot curve, concentration gradient curve, pH response interval and time response interval of the synthesized fluorescent probe were studied by UV-Vis absorption spectrometer and fluorescence spectrophotometer.

1.6.3 Synthetic route

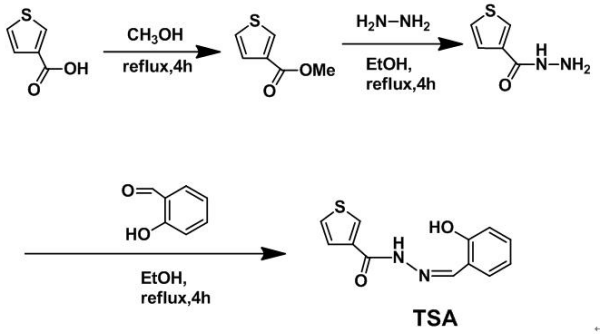

Scheme. 1 synthesizing scheme of **TSA**

Chapter 2 Experimental Section

2.1 Experimental objective

1. Synthesizing the target compound (**TSA**) with designed route that followed the principles of convenience, efficiency, high yielding and low cost.

2. Skillfully master the chemical drawing software (Chem-Draw) and others.

3. Master the operation of corresponding instruments and equipment related to my

work.

4. study the mechanisms behind the instruments and master the skill of analyzing spectrum.

2.2 Characterization methods

High-resolution mass spectrometry (HR-MS) was performed by Agilent 6510 Accurate-Mass Q-TOF LC / MS system. Infrared measurement is performed in the range of 4000-400 cm^{-1} of a Bruker ALpHA FT-IR spectrometer using KBR tablet technology. ^{1}H NMR(400 MHz) Nuclear magnetic resonance hydrogen spectrum and ^{13}C (100 MHz) NMR Nuclear magnetic resonance carbon spectrum recording were recorded using a Bruker Avance II 400 with TMS Tetramethylsilane (δ = 0.00 ppm) was used as the internal standard. The UV-Vis absorption spectra were performed by a Shimadzu UV-2600 at room temperature and the fluorescence measurements were performed at room temperature on a Hitachi F-4600 fluorescence spectrophotometer at a scan rate of 2400 nm/min, and the excitation wavelength was 290 nm, the excitation and emission slits were set to 5/5 nm, respectively.

2.3 Reagents and Apparatus

2.3.1 Reagents

Table 2-1. Reagents used in this experiment.

Reagents	**Purity**	**Manufacturer**
3-Thiophenezoic acid	99.0% (AR)	JiuDing Chemical Factory
2-hydroxyl-4-(N,Ndiethyl)aminobenzaldehyde	99.0% (AR)	JiuDing Chemical Factory
Hydrazine	80% (AR)	Tianjin KeMiOu Chemical Reagent Co Ltd.
Ethyl acetate	98.0% (AR)	Tianjin Fuyu Fine Chemical Co, Ltd.

Petroleum Ester	98.0% (AR)	Tianjin Fuyu Fine Chemical Co, Ltd.
DMSO	99.0% (AR)	Tianjin Fuyu Fine Chemical Co, Ltd.
Ethanol	99.7% (AR)	Tianjin Fuyu Fine Chemical Co, Ltd.
Methol	99.7% (AR)	Tianjin Fuyu Fine Chemical Co, Ltd.
$MgSO_4$	99.5% (AR)	Tianjin Damao Chemical Reagent Factory
$NaHCO_3$	99.5% (AR)	Tianjin Guangcheng Chemical Reagent Co Ltd.
NaCl	99.0% (AR)	TTianjin Guangcheng Chemical Reagent Co Ltd.
$NaNO_3$	99.5% (AR)	Aladdin Chemical Reagent Co, Ltd.
$AgNO_3$	99.8% (AR)	Shanghai Siyu Chemical Co, Ltd.
KNO_3	99.8% (AR)	Shanghai Siyu Chemical Co, Ltd.
$Zn(NO_3)_2·6H_2O$	98.0% (AR)	Aladdin Chemical Reagent Co, Ltd.
$Co(NO_3)_2·6H_2O$	98.0% (AR)	Aladdin Chemical Reagent Co, Ltd.
$Ni(NO_3)_2·6H_2O$	98.0% (AR)	Aladdin Chemical Reagent Co, Ltd.
$Ca(NO_3)_2·4H_2O$	98.0% (AR)	Aladdin Chemical Reagent Co, Ltd.
$Al(NO_3)_3·9H_2O$	98.0% (AR)	Aladdin Chemical Reagent Co, Ltd.
$Cu(NO_3)_2·3H_2O$	98.0% (AR)	Aladdin Chemical Reagent Co, Ltd.
$Cd(NO_3)_2·4H_2O$	98.0% (AR)	Aladdin Chemical Reagent Co, Ltd.
$Fe(NO_3)3·9H_2O$	98.0% (AR)	Aladdin Chemical Reagent Co, Ltd.
$Hg(NO_3)_2·H_2O$	98.0% (AR)	Aladdin Chemical Reagent Co, Ltd.
$Pb(NO_3)_2$	99.0% (AR)	Aladdin Chemical Reagent Co, Ltd.
$CrCl_3·6H_2O$	99.5% (AR)	Aladdin Chemical Reagent Co, Ltd.
$FeCl_2·4H_2O$	99.0% (AR)	Aladdin Chemical Reagent Co, Ltd.

2.3.2 Apparatus

Table 2-2. Instruments used in this experiment.

Name	Model	Manufacturer
Vacuum Drier	DZF-6030A	Shanghai yayong technology co.LTD.
Rotary Evaporator	RE-52A	Shanghai yayong biochemical instrument factory
Vacuum Drier	DZF-6030A	Shanghai yayong technology co.LTD.
Electronic Balance	AL204	Mettler Toledo
Constant Temperature Heating Magnetic Stirrer	DF-101S	gongyi yingyu instrument factory
Nuclear Magnetic Resonance Spectrometer	AVANCE II 400	USA Bruker
Fourier Infrared Spectrometer	IRPrestige-21	Japan shimazu company
Uv-Visible Absorption Spectrometer	UV2600	Shimadzu
Fluorescence Spectrophotometer	HITACHI F-4600	HITACHI
High Resolution Mass Spectrometer	Agilent 6510	Agilent

2.4 Experiment Contents

2.4.1 preparation of testing solution

A suitable amount of compound **TSA** was dissolved in DMSO to obtain its reserve solution (1.0 mM), and deionized water was used to dilute metal ions (Al^{3+}, Cd^{2+}, Cr^{3+}, Fe^{2+}, Na^{+}, K^{+}, Ag^{+}, Ca^{2+}, Cu^{2+}, Ba^{2+}, Co^{2+}, Ni^{2+}, Pb^{2+}, Fe^{3+}, Hg^{2+}, Mg^{2+}, Sr^{2+}, Zn^{2+}) to 1.0 mM to obtain the stock solution.Then, they were all prepared to be

analytical solution (10 μM) by DMSO/H_2O (1:1, V/V) solution. Afterwards, making concentration gradient (0-5μM) of the metal ion solution. All the experiments were done at room temperature.

2.4.2 Cell culture

Hela (cervical cancer cells) cell lines were maintained in DMEM medium supplemented with FBS (10%), and glutamine (5%). Cells were grown in a humidified incubator at 37 °C, 5% CO_2, and 95% air. Hela cell line were seeded onto T-75 flask and incubated with **TSA** (10.0 μM) at same condition while others further incubated with Al^{3+} for 30 mins and longer. Then, they all were rinsed with PBS for three times before took bioimaging tests with Laser scanning confocal microscopy[18].

2.4.3 Synthesising of **TSA**

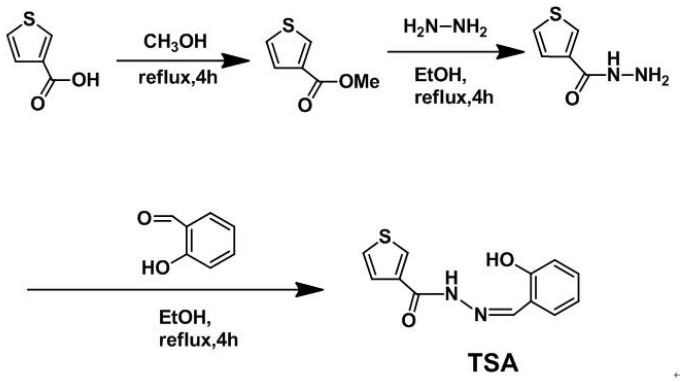

Scheme 1 synthesizing scheme of **TSA**

3-thiophenezoic acid (1.0g, 7.8mmol) was dissolved in methanol,（15ml）added with 1% concentrated sulfuric acid, refluxed for 4h, decompressed and concentrated, washed with saturated sodium hydrogen carbonate and extracted with ethyl acetate, decompressed and concentrated, resulting in yellow oily liquid. (1g, 7.04 mmol, yield, 90%)[21] Methyl-3-thiophenecarboxylate (1.0g, 7.04 mmol) was dissolved in ethanol (15ml), hydrazine hydrate (0,96g, 6.70mmol) was added, refluxed for 4h,

decompressed and concentrated, and washed with ethanol to obtain white crystalline solid (0.96g,yield,96%). Thiophene-3-carbohydrazide (0,96g,6.70mmol), and salicylaldehyde (0.82g, 6.70mmol) was dissolved in ethanol and heated to reflux for 4h. After cooling to room temperature, the desired TS (1.80g,yield, 90%) product, a yellow solid, was obtained by simple filtration and collection.

^{1}H NMR (400 MHz, DMSO-d6, ppm): δ 11.85 (s, 1H), 11.13 (s, 1H), 8.52 (s, 1H), 8.23 (s, 1H), 7.61 (d, J = 8.0 Hz, 1H), 7.52 (d, J = 4.0 Hz, 1H), 7.47 (d, J = 4.0 Hz, 1H), 7.21 (t, J = 16.0 Hz, 1H), 6.83 (t, J = 12.0 Hz, 2H); ^{13}C NMR (100 MHz, DMSO-d6, ppm): δ 158.32, 157.34, 147.62, 135.49, 131.29, 130.10, 129.31, 127.25, 126.82, 119.30, 118.71, 116.35; FTIR (KBr, cm^{-1}): ν = 3425 (O-H), 3223 (N-H), 1622 (C=O), 1589 (C=N), 1512 (C=C); HRMS (ESI): m/z [M+H]+ calcd. for: $C_{12}H_{10}N_2O_2S$: 247.0541, found: 247.0538. The characterization figures can be found in the electronic supplementary information (Fig. S1–S4).

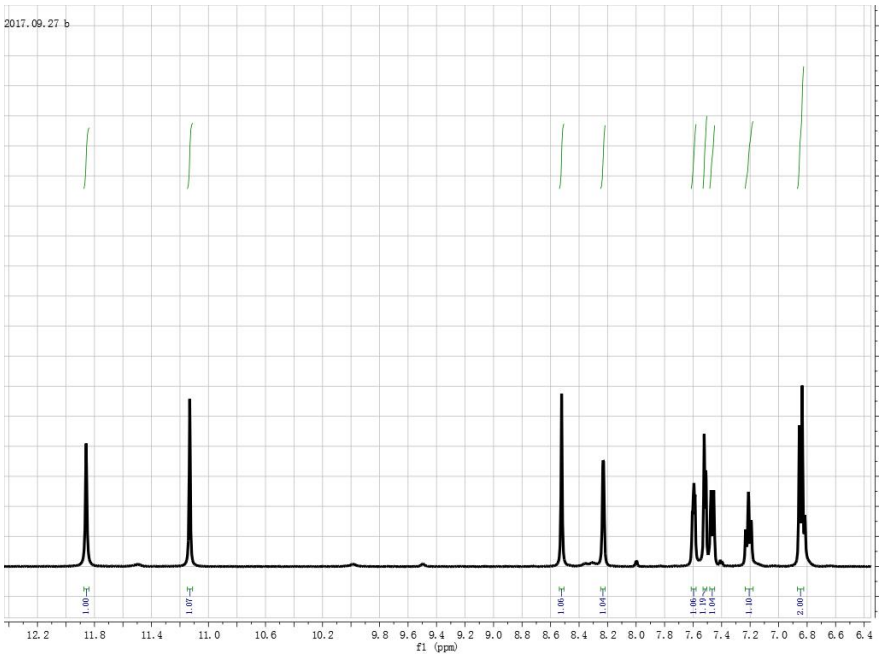

Figure S1 The ^{1}H NMR of **TSA**

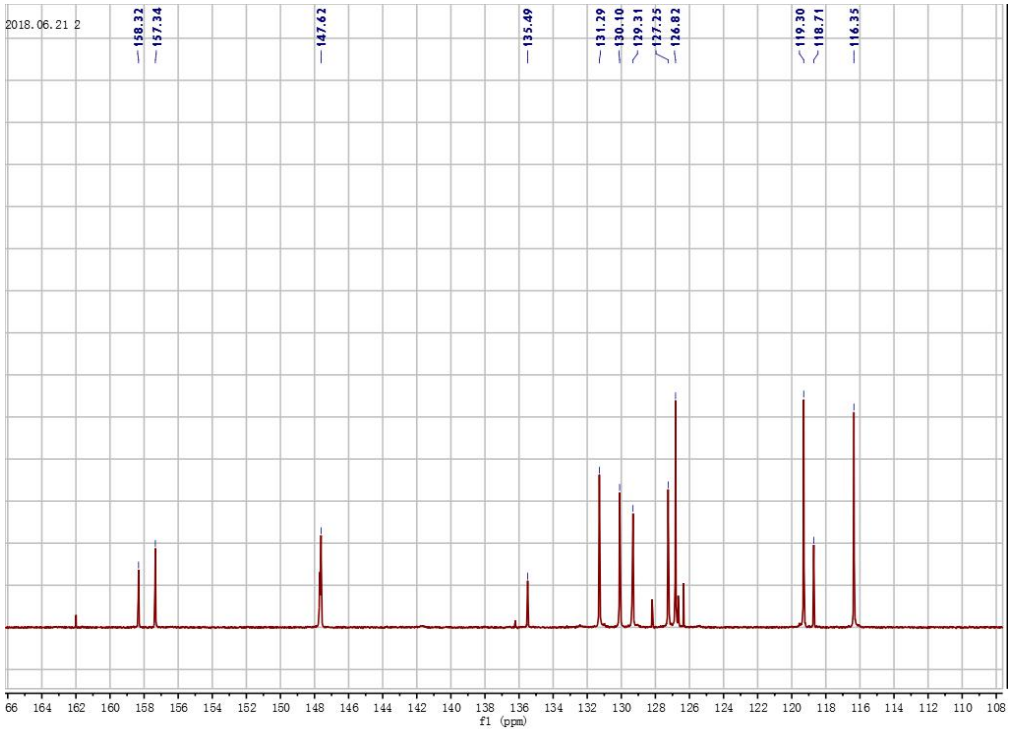

Figure S2 The ^{13}C spectra of **TSA**

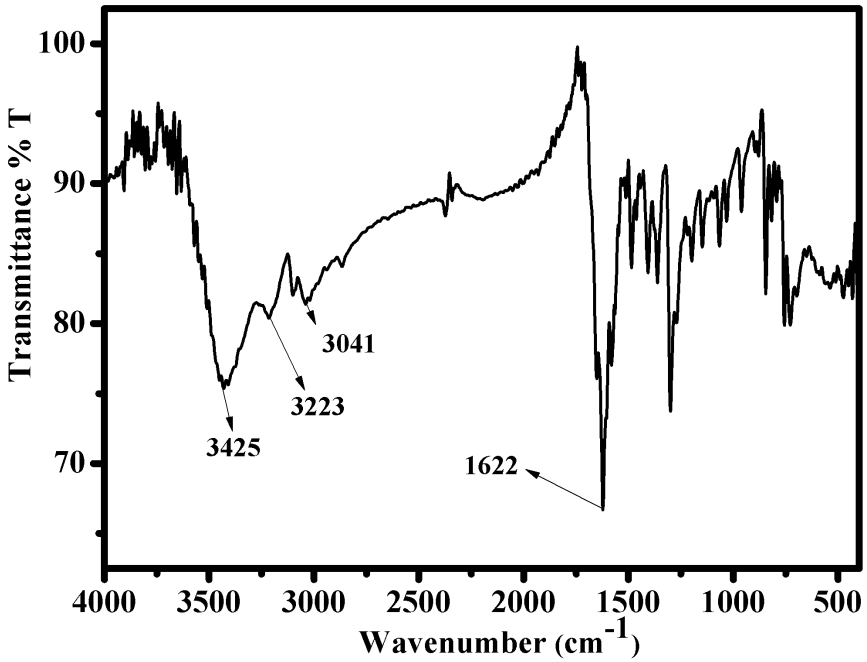

Figure S3 The IR spectra of **TSA**

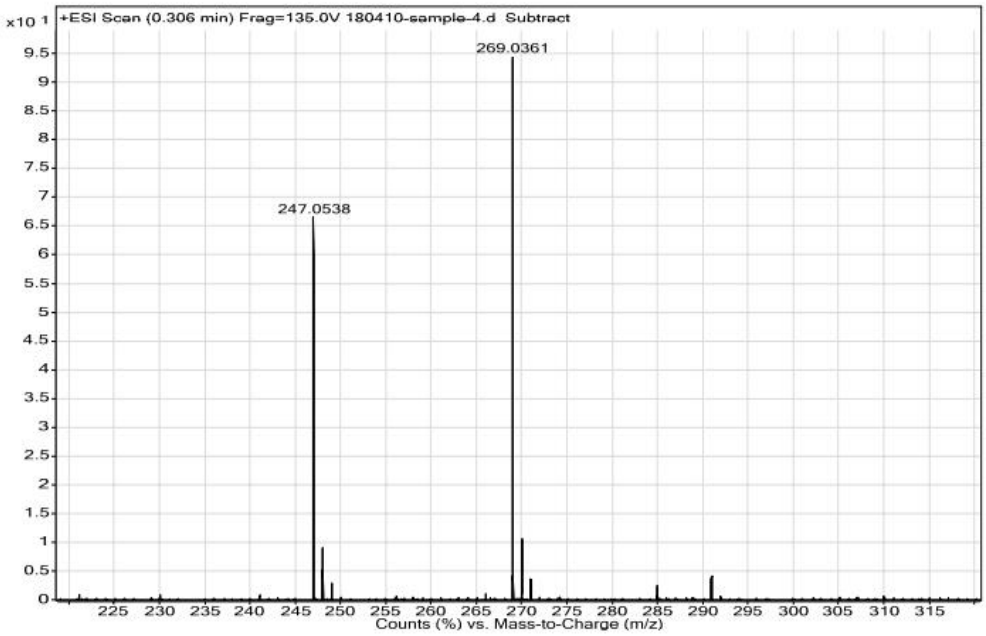

Figure S4 The HRMS spectra of **TSA**

Chapter 3 Result and discussion

3.1 High Fluorescence selectivity to Al^{3+}

In order to explore the selectivity of **TSA** to Al^{3+} ions in DMSO/H2O (1/1, v/v) solution, a series of metal ions (Al^{3+}, Cd^{2+}, Cr^{3+}, Fe^{2+}, Na^{+}, K^{+}, Ag^{+}, Ca^{2+}, Cu^{2+}, Ba^{2+}, Co^{2+}, Ni^{2+}, Pb^{2+}, Fe^{3+}, Hg^{2+}, Mg^{2+}, Sr^{2+}, Zn^{2+}) (2.0 equiv.) were respectively added to 10 μM of the **TSA** under the excitation wavelength (365 nm), and the UV-Vis absorption and fluorescence spectra came out. The graph (Fig 3.1) gives information of the reaction between **TSA** and metal ions. As it can be seen that only Al^{3+} ions caused a large absorption band centered at 465 nm (absorbance increased

around 300 folds) with a distinct color change from colorless to naked-eye observed blue. However, neither the color nor the fluorescence intensity display a clear change As displayed in Fig.3-1 when others ions were added to **TSA** analytical solution.These observations illustrate that the flurescent sensor **TSA** has a high selectivity to Al^{3+}.

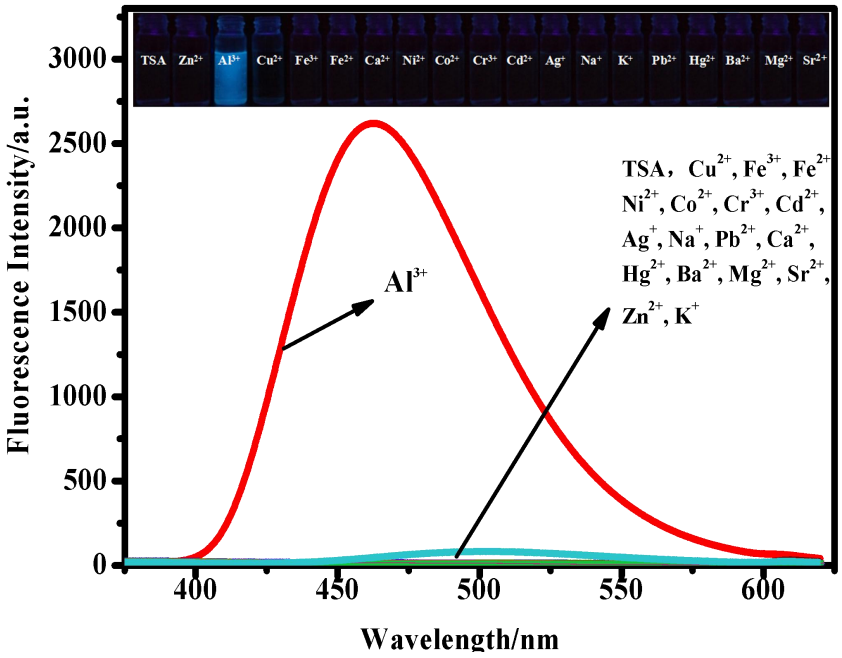

Fig. 3-1 Fluorescence spectra of **TSA** (10 μM) upon the addition of various metal ions (2.0 equiv.) in DMSO/H_2O (1/1, v/v) solution; **Inset**: The colors of **TSA** upon addition of various metal ions under 365 nm UV lamp

3.2 Anti-interference performance of TSA

An excellent fluorescent probe possess strong competitiveness towards others, and it reacts stronger than its interference ions. To investigate the interference effect of the coexisting ions during the Al^{3+} ions detection, a series of metal ions (Al^{3+}, Cd^{2+}, Cr^{3+}, Fe^{2+}, Na^{+}, K^{+}, Ag^{+}, Ca^{2+}, Cu^{2+}, Ba^{2+}, Co^{2+}, Ni^{2+}, Pb^{2+}, Fe^{3+}, Hg^{2+}, Mg^{2+}, Sr^{2+}, Zn^{2+}) (2.0 equiv.) were respectively added to the solution of **TSA**-Al^{3+}, and then the fluorescence spectra were carried out, respectively (Fig. 3-2). The bar chart shows that these competitive ions exerted little influence on the absorbance and emission intensity **TSA**-Al^{3+} solution,which indicating that **TSA** had outstanding anti-interference ability for fluorimetric detection of Al^{3+} in aqueous media.

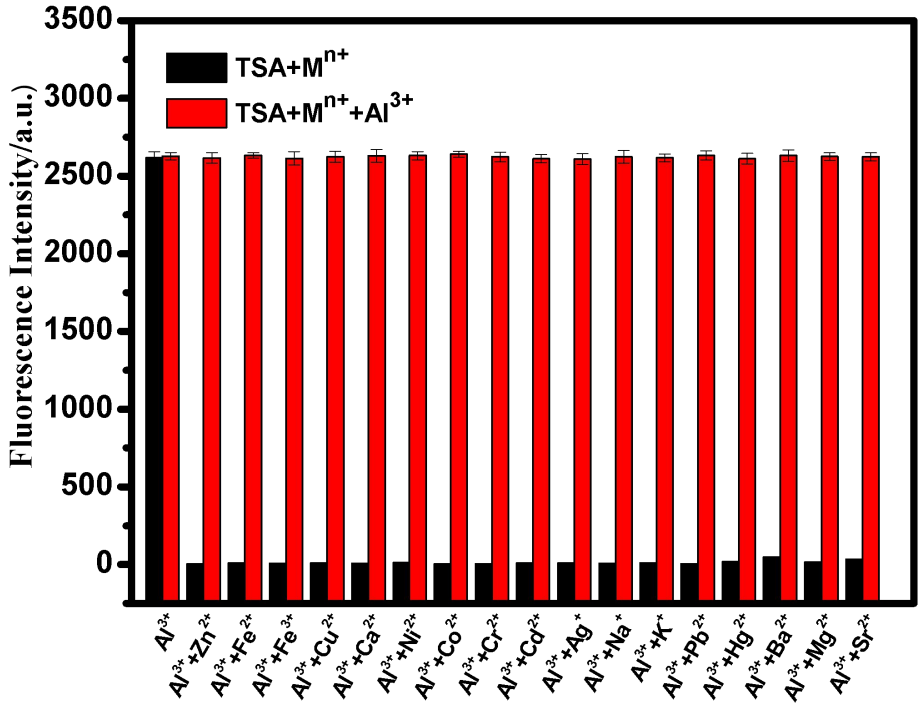

Fig 3-2 Fluorescence intensity changes of **TSA** (10 μM) in DMSO/H_2O (1/1, v/v) solution upon addition of 2.0 equiv. various metal ions (black bars). The red bars represent the change in absorbance when 2.0 equiv. Al^{3+} ion was added to the mixture of **TSA** (10 μM) and 2.0 equiv. of other metal ions, respectively.

3.3 The sensitivity of TSA to Al^{3+}

The fluorescence titration were carried out for the sake of exploring how **TSA** can detect Al^{3+} quantitatively in DMSO/H2O (1/1, v/v) solution, Al^{3+} (0–2.0 equiv.) were added to **TSA** solution. The graph in Fig 3.31 Displayed an gradual fluorecent enhancement at 450 nm with the concentration increase of Al^{3+}(0–1.0 equiv.). The spectra of **TSA** vs. concentration of Al^{3+} (inserted in the graph) presents a linear relationship between the flurescent intensity of the sensor **TSA** and aluminium ion concentration (0–1.0 equiv.). The fluoresent titration line suggests a 1:1 binding stoichiometry between **TSA** and Al^{3+}.

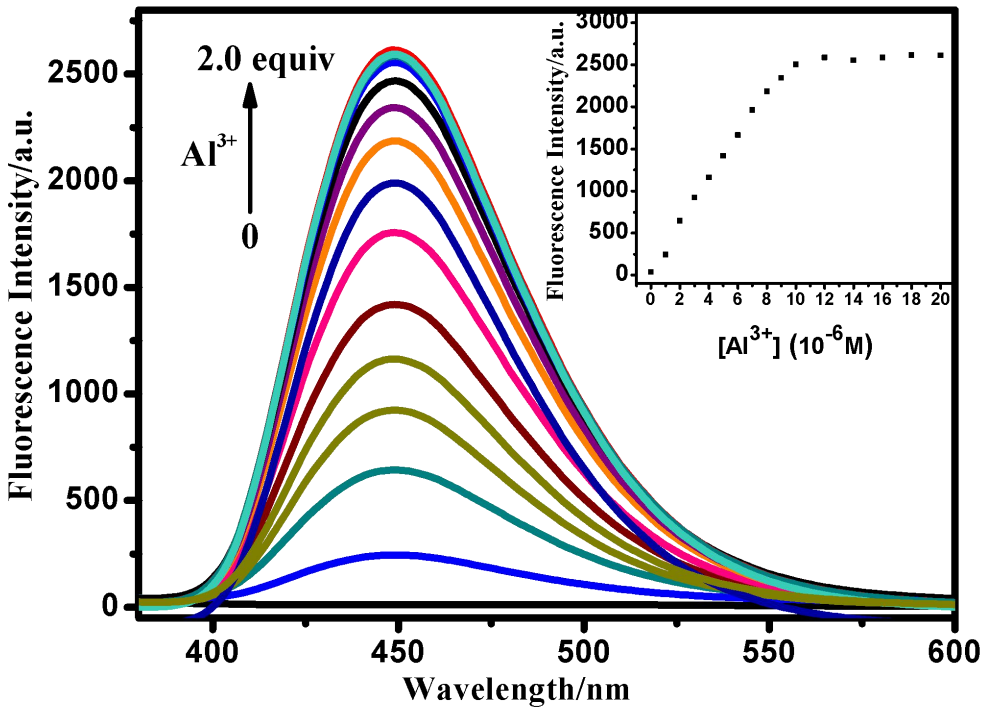

Fig. 3-3 Fluorescence response of **TSA** (10 μM) on addition of Al^{3+} (0–2.0 equiv.) in DMSO/H_2O (1/1, v/v) solution; The inset shows fluorescence intensity of **TSA** as a function of Al^{3+} concentration at 450 nm.

To further confirm the ratio between **TSA** and Al^{3+}concentration, Job's plot for **TSA**-Al^{3+} system (Fig. 3.3) was designed. As it can be seen from the graph, The maximum absorbance intensity at 450 nm appeared when the molar fraction of Al^{3+}/ **TSA**-Al^{3+} was 0.5, which indicated that the 1:1stoichiometry was the possible binding mode of **TSA** with Al^{3+} ions. Besides, the calculating results present that the fluorescent intensity of **TSA** was linearly proportional to the Al^{3+} with a correlation coefficient of 0.98887 (Fig. 3-3).

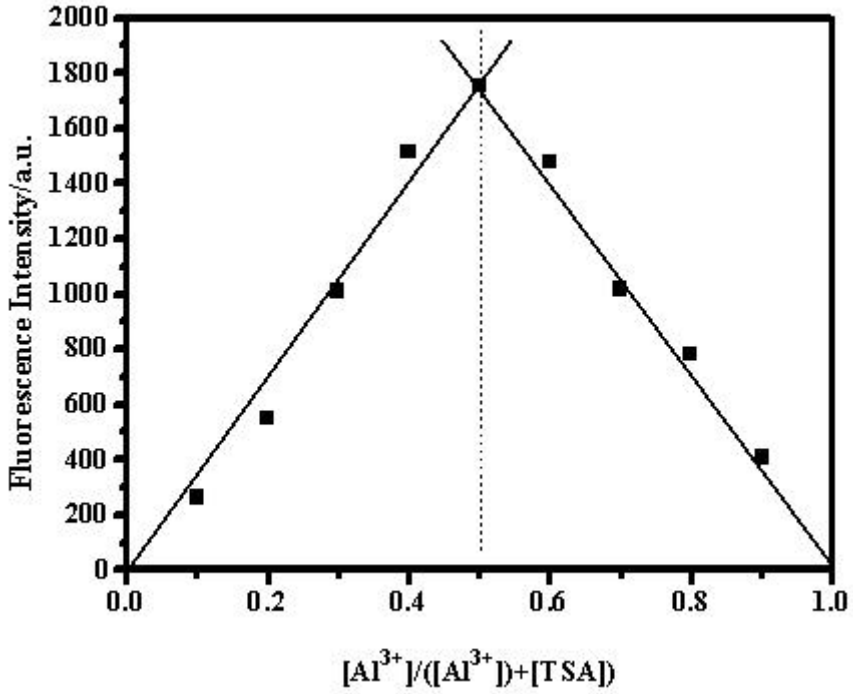

Fig. 3-4 Job's plot for **TSA**-Al^{3+} system

3.4 Limited of detection of TSA-Al^{3+}

Small limited of detection means fast recognition and high sensitivity. According to the titration data, the Limited of detection (LOD) of **TSA**-Al^{3+} was calculated to be 8.36×10^{-9} M by (LOD = 3 δ /slope) (where δ is the 20 times of standard deviation of the blank **TSA** solution, and S is the slope of the intensity ratio versus sample concentration plot), which is lower than most probes' in previous work, indicating that the probe is sensitive enough to detect Al^{3+} in living cells .

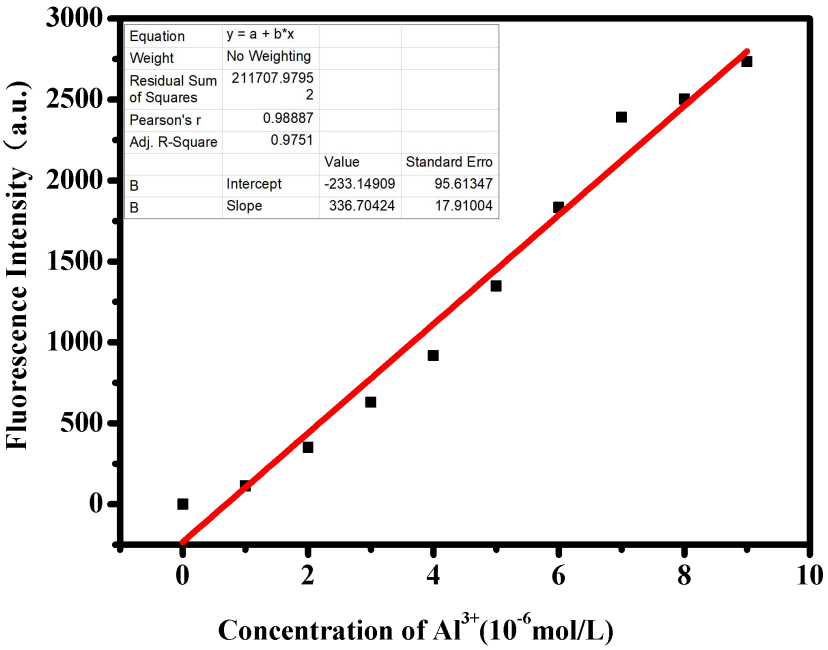

Fig. 3-5 Fluorescence intensity at 463 nm of sensor **TSA** upon gradual addition of Al^{3+} (0–10 μm)

3.5 Calculation of the binding association constant

The association constant was calculated using the BenesiHildebrand plot (or a double-reciprocal plot) as shown in Eq. 1

$$\frac{1}{A-A_0}=\frac{1}{K_a\times(A_{max}-A_0)\times[Al^{3+}]}+\frac{1}{A_{max}-A_0} \quad (1)$$

where; A is the experimentally measured absorption intensity, A0 is the absorption intensity of free **TSA**, and A_{max} is the saturated absorption intensity of the **TSA**-Al^{3+} complex. The association constant (Ka) was graphically evaluated by plotting $1/[A - A_0]$ versus $1/[Al^{3+}]$, as shown in Fig 3-6[27].

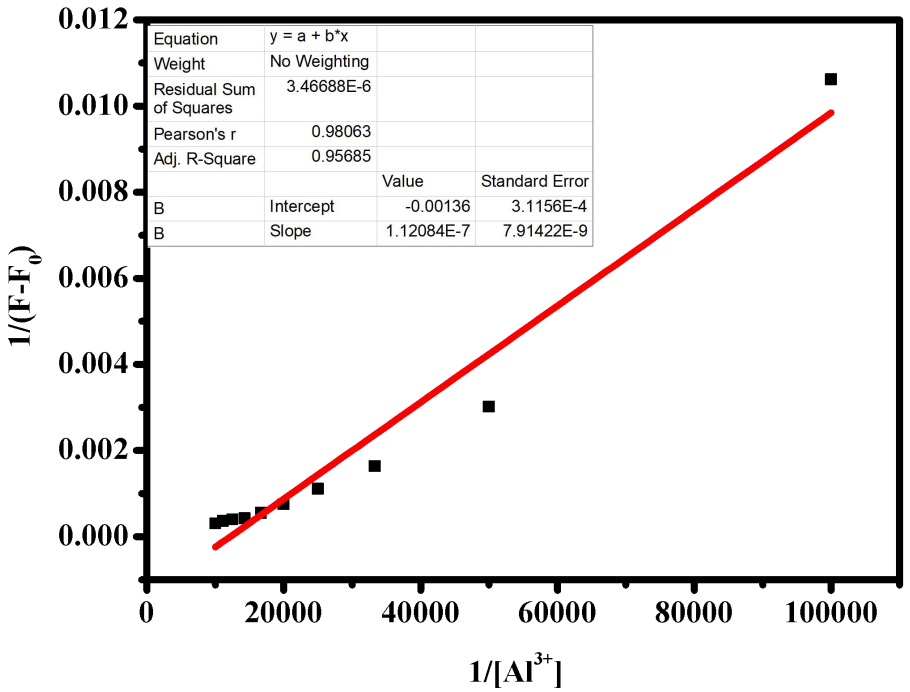

Fig. 3-6 Benesi-Hildebrand plot for determination of binding constant of **TSA** (10 μM) with Al^{3+} ion in DMSO/H_2O (1/1, v/v) solution.

From the obtained linear relationship, the binding constant (Ka) was calculated which equal to 5.14×10^4 M^{-1}. (R = 0.98063) according to the graph.

3.6 pH Responses of Sensor TSA to Al^{3+}

A qualified fluorescent probe should possess applicability which is the fluorescent test that can be done in a wide range of PH. In order to study the practice of **TSA**, the PH response was presented as it is an important factor in evaluation. Fluorescent sensors based on electron donor and acceptor systems could be affected by the testing environment. To further study the suitable working pH range of **TSA**, a series of **TSA** and **TSA**-Al^{3+} solutions differ in pH values (1.0-14.0) were prepared, and the fluorescence spectra were carried out (Fig. 3-7). the graph displayed a relative fluctuation of fluorescent intensity in this PH range under DMSO/H_2O (1/1 V/V). Besides, the fluorescent intensity changes of **TSA** (10 μm) at 460 nm is not big, and the figure almost keeps constant in the range (pH 3.0-11.0), which indicated that **TSA** could be used as a detector for Al^{3+} in the working pH span of 3–11 by the fluorescence measurement.

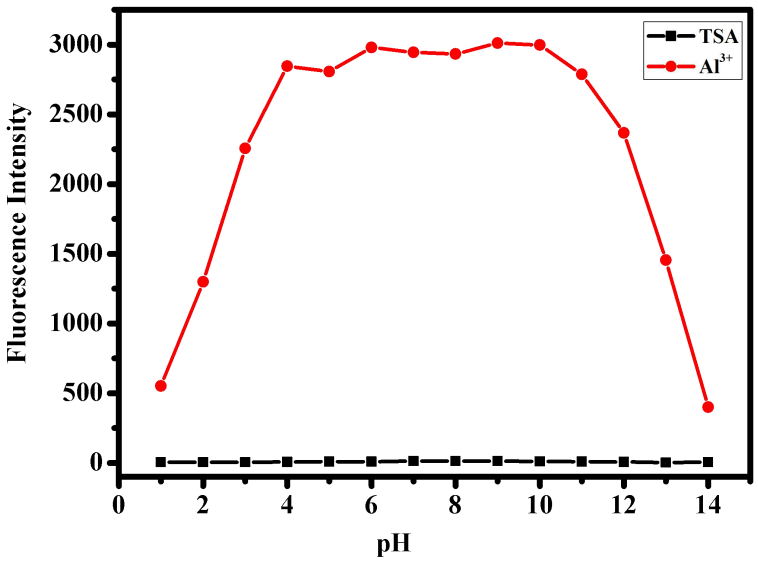

Fig. 3-7 Effect of pH on the fluorescence intensity of **TSA** (10 μM) in absence and presence of Al^{3+} ion.

3.7 The time response of TSA to Al^{3+}

The response time is another vital analytical characteristic (the sensitivity of **TSA**) of a fluorescent probe. In this part of the work, the time study on fluorescence response of **TSA** (10 μM) to Al^{3+} ions (2.0 equiv.) was measured in DMSO/H_2O (1/1, v/v) solution. As shown in Fig. 3-8, the fluorescence intensity of the **TSA**-A^{3+} system present a significant enhancement in a few seconds. The fluorescence intensity at 460 nm increased with time and reached a high point at a certain time (20 s) and then level off over a long period, suggesting that the binding process between **TSA** and Al^{3+} is very fast and quite stable, which can be further use for practical applications.

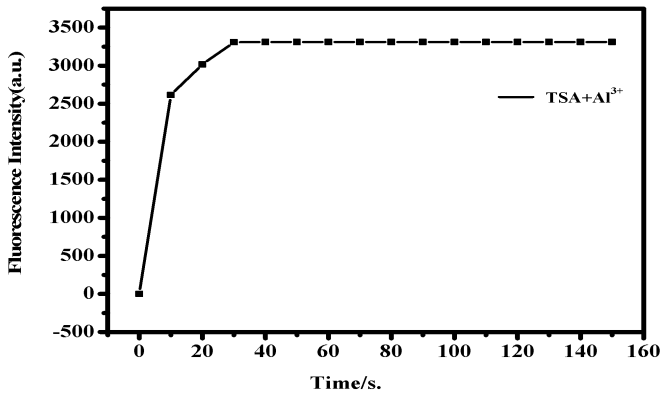

Fig. 3-8 Time resolved fluorescence profile of **TSA** (10 μM) upon the addition of Al^{3+} ion (2.0 equiv.) in DMSO/H_2O (1/1, v/v) solution.

3.8 Cell imaging study

Hela (cervical cancer cells) cell lines were maintained in DMEM medium supplemented with FBS (10%), anti-mold agent (1%), and glutamine (5%). Cells were grown in a humidified incubator at 37 oC, 5% CO2, and 95% air with **TSA** (10.0 μM) for 60 mins. Then, the cell was rinsed with PBS three times before took bioimaging tests with Laser scanning confocal microscopy. As can be seen from the picture (scanned picture) and b (Bright-field image), no clear color change was observed after incubation with only **TSA**. Afterward, carried out the second test, the Hela cell was incubated with **TSA** for 30 mins under the same environment and added Al^{3+} for another 30 mins, the image (c) displayed a blue color, which implies that intracellular complexing occurred. The image (d) shows an intense blue fluorescence, and the fluorescent intensity did not change for some time. All these phenomena indicate that the **TSA** possesses low cytotoxicity in the living HeLa cells. The fluorescence imaging experiments indicated that **TSA** was cell-permeable and could be used as an effective intracellular Al^{3+} imaging agent[18].

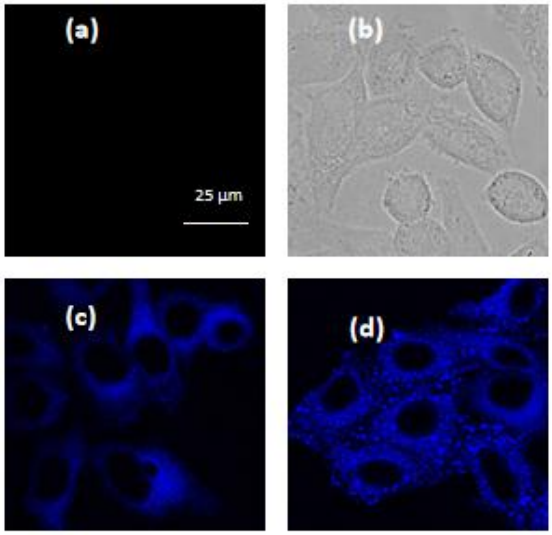

Fig 3-9 Fluorescence microscope images of the HeLa cells. After incubation with the **TSA** (10 μM) for 60 min (**a**); Bright-field images (**b**); after incubation with the **TSA** (10 μM) for 30 min and then further incubated with Al^{3+} (10 μM) for 30 min (**c**) and 60 min (**d**).

Chapter 4 Conclusion

In summary, we have developed a new colorimetric fluorescent sensor **TSA** based on thiophene derivatives. The sensor has a significant fluorescence enhancement response to Al^{3+}, also, **TSA**-Al^{3+} system showed a complete insensitivity to the pH in the range 3–11, maintaining intact their fluorescence capability. Competitive experiments show that **TSA** has high fluorescence selectivity for Al^{3+} **TSA** has a high affinity for Al^{3+} with detection limits of 8.36 $\times 10^{-9}$M and the binding constant (ka) between **TSA** and Al^{3+} is 5.14 x 10^4 M^{-1}. Besides, the sensor **TSA** has been successfully applied to the quantification of Al^{3+} in actual water and cell samples, with good precision and accuracy. Fluorescence imaging experiments show the practical application of the **TSA** sensor to detect Al^{3+} in living HeLa cells. The work provides a new method with the simple synthetic route and low cost for ultra-sensitive, selective, quantitative, and micro-detection of Al^{3+} in environmental and biological systems.

Bibliography

[1] M. F. Kramer and M. D. Heath, "Aluminium in allergen-specific subcutaneous immunotherapy--a German perspective," *Vaccine,* vol. 32, no. 33, pp. 4140-8, Jul 16 2014.

[2] V. R. Bitra, D. Rapaka, N. Mathala, and A. Akula, "Effect of wheat grass powder on aluminum induced Alzheimer's disease in Wistar rats," *Asian Pacific Journal of Tropical Medicine,* vol. 7, pp. S278-S281, 2014.

[3] J. Fu, Y. Chang, B. Li, X. Wang, X. Xie, and K. Xu, "A dual fluorescence probe for Zn(2+) and Al(3+) through differentially response and bioimaging in living cells," *Spectrochim Acta A Mol Biomol Spectrosc,* vol. 225, p. 117493, Jan 15 2020.

[4] J. C. Berrones-Reyes, C. C. Vidyasagar, B. M. Muñoz Flores, and V. M. Jiménez-Pérez, "Luminescent molecules of main group elements: Recent advances on synthesis, properties and their application on fluorescent bioimaging (FBI)," *Journal of Luminescence,* vol. 195, pp. 290-313, 2018.

[5] Y. Liu *et al.*, "A naphthalimide–rhodamine ratiometric fluorescent probe for Hg2+ based on fluorescence resonance energy transfer," *Dyes and Pigments,* vol. 92, no. 3, pp. 909-915, 2012.

[6] J. Y. Noh *et al.*, "Solvent-dependent selective fluorescence assay of aluminum and gallium ions using julolidine-based probe," *Dyes and Pigments,* vol. 99, no. 3, pp. 1016-1021, 2013.

[7] H. Cho, J. B. Chae, and C. Kim, "A thiophene-based blue-fluorescent emitting chemosensor for detecting indium (III) ion," *Inorganic Chemistry Communications,* vol. 97, pp. 171-175, 2018.

[8] J. Berrones-Reyes *et al.*, "Novel fluorescent Schiff bases as Al3+ sensors with high selectivity and sensitivity, and their bioimaging applications," *Materials Chemistry and Physics,* vol. 233, pp. 89-101, 2019.

[9] Z.-D. Sun, M. He, K. Chaitanya, and X.-H. Ju, "Theoretical studies on D-A-π-A and D-(A-π-A)2 dyes with thiophene-based acceptor for high performance p-type dye-sensitized solar cells," *Materials Chemistry and Physics,* vol. 248, 2020.

[10] T. M. Elmorsi, T. S. Aysha, O. Machalický, M. B. I. Mohamed, and A. H. Bedair, "A dual functional colorimetric and fluorescence chemosensor based on benzo[f]fluorescein dye derivatives for copper ions and pH; kinetics and thermodynamic study," *Sensors and Actuators B: Chemical,* vol. 253, pp. 437-450, 2017.

[11] L. Yang *et al.*, "Red turn-on fluorescent phenazine-cyanine chemodosimeters for cyanide anion in aqueous solution and its application for cell imaging," *Sensors and Actuators B: Chemical,* vol. 203, pp. 833-847, 2014.

[12] F.-W. Gao, Q.-C. Liang, and H.-L. Xu, "Straight Z and twisted E isomers from triphenylamine derivatives: Intramolecular charge transfer and second-order nonlinear optical response," *Journal of Molecular Liquids,* vol. 311, 2020.

[13] G.-J. Kang, S. He, H.-Y. Cheng, and X.-F. Ren, "Enhanced intramolecular charge transfer of organic dyes containing hydantoin donor: A DFT study," *Journal of Photochemistry and Photobiology A: Chemistry,* vol. 383, 2019.

[14] P. Guan, B. Yang, and B. Liu, "Fabricating a fluorescence resonance energy transfer system with AIE molecular for sensitive detection of Cu(II) ions," *Spectrochim Acta A Mol Biomol Spectrosc,* vol. 225, p. 117604, Jan 15 2020.

[15] J. W. Nugent, H. Lee, J. H. Reibenspies, H.-S. Lee, and R. D. Hancock, "Effects of anion coordination on the fluorescence of a photo-induced electron transfer (PET) sensor complexed with metal ions," *Polyhedron,* vol. 130, pp. 47-57, 2017.

[16] A. Tang, Y. Yin, Z. Chen, C. Fan, G. Liu, and S. Pu, "A multifunctional aggregation-induced emission (AIE)-active fluorescent chemosensor for detection of Zn2+ and Hg2+," *Tetrahedron,* vol. 75, no. 36, 2019.

[17] K. Mahesh and S. Karpagam, "Thiophene-thiazole functionalized oligomers-excellent fluorescent sensing and selective probe for copper and iron ion," *Sensors and Actuators B: Chemical,* vol. 251, pp. 9-20, 2017.

[18] N. Vijay, S. P. Wu, and S. Velmathi, "Turn on fluorescent chemosensor containing rhodamine B fluorophore for selective sensing and in vivo fluorescent imaging of Fe3+ ions in HeLa cell line and zebrafish," *Journal of Photochemistry and Photobiology A: Chemistry,* vol. 384, 2019.

Acknowledgments

In this work, I got support from my tutor Mrs. Niu Qingfen, senior student Yin Pengchen and my fellow students in the same lab. I appreciate them all for their helpful discussion and valuable comments whenever I need help. Hereby, thanks for meticulous guidance from my teachers and warm encouragement from my friends throughout my college life. I believe the knowledge and skills I gained would be practical and helpful in my future work and life.